Quaternary Geochronology 67 (2022) 101232

Contents lists available at ScienceDirect

Quaternary Geochronology

journal homepage: www.elsevier.com/locate/quageo

Bayesian estimates of marine radiocarbon reservoir effect in northern Iberia during the Early and Middle Holocene

Asier García-Escárzaga [a,b,c,*], Igor Gutiérrez-Zugasti [d], David Cuenca-Solana [d,e], Manuel R. González-Morales [d], Christian Hamann [f], Patrick Roberts [b,g], Ricardo Fernandes [b,h,i,**]

[a] Departamento de Ciencias Humanas, Universidad de La Rioja, Edificio Vives, C/ Luis de Ulloa, 2, 26004, Logroño, Spain
[b] Department of Archaeology, Max Planck Institute for the Science of Human History, Kahlaische Str. 10, 07745, Jena, Germany
[c] Departamento de Geografía, Prehistoria y Arqueología, Universidad del País Vasco (UPV/EHU), C/ Tomás y Valiente s/n, 01006, Vitoria-Gasteiz, Spain
[d] Instituto Internacional de Investigaciones Prehistóricas de Cantabria (Universidad de Cantabria, Gobierno de Cantabria, Grupo Santander), Universidad de Cantabria, Edificio Interfacultativo, Avda. Los Castros s/n, 39005, Santander, Spain
[e] Centre de Recherche en Archéologie, Archeosciences, Histoire (CReAAH), UMR-6566, Université de Rennes 1, Rennes, France
[f] Leibniz Laboratory for Radiometric Dating and Stable Isotope Research, Kiel University, Max- Eyth-Str. 11–13, 24118, Kiel, Germany
[g] School of Social Sciences, University of Queensland, St Lucia, Queensland, 4072, Australia
[h] School of Archaeology, University of Oxford, 1 South Parks Road, Oxford, OX1 3TG, United Kingdom
[i] Faculty of Arts, Masaryk University, Arne Nováka 1, 602 00, Brno-střed, Czech Republic

ARTICLE INFO

Keywords:
Mesolithic
Shell middens
Cantabrian region
Marine radiocarbon reservoir effect
Bayesian modelling
Marine environments
8.2 ka event

ABSTRACT

Reconstructing the past variability of marine radiocarbon reservoir effects (MRE) is crucial for generating reliable chronologies for marine species and their consumers. We investigated the temporal MRE variability at the Early-to Mid-Holocene site of El Mazo (Asturias, northern Spain) by using a combination of new and previously published radiocarbon measurements on marine and terrestrial samples. The El Mazo site is characterized by overall well-defined archaeological layers of unknown occupation length with the predominant presence of two mollusc species (*Patella vulgata* Linnaeus, 1758 and topshell *Phorcus lineatus* [da Costa, 1778]) which were analysed for radiocarbon measurements. We employed the recently released IntCal20 calibration curve for the northern hemisphere and Bayesian modelling to reconstruct the site's chronology and temporal variability in MREs according to mollusc species. Obtained radiocarbon modelling results, although the estimate precision is not high, reveal a temporal variability in MREs that can be interpreted in view of known past climatic and environmental events such as the 8.2 ka event. The results also revealed differences in MREs according to mollusc species, which need to be taken into account in future chronological modelling. Overall, our results provide reference MRE values for the study of chronologies in northern Iberia during the Early-to Mid-Holocene. In this respect, a non-conservative ΔR reference for local marine samples dating earlier than c. 8.1 ka cal BP is −238 ± 28 ^{14}C years.

1. Introduction

Radiocarbon measurements of marine shells are increasingly employed for establishing the absolute chronologies of archaeological sites (Bosch et al., 2015; Gutiérrez-Zugasti et al., 2018a; Zilhão et al., 2010) and are particularly useful for stratigraphic sequences where shells represent the majority of the archaeological record (Mannino et al., 2007; Hardy et al., 2016; Hausmann et al., 2019). However, the radiocarbon age of marine shells can appear significantly older than the actual time of deposition since marine species are typically depleted in their ^{14}C content when compared to contemporary terrestrial samples in equilibrium with the atmosphere. Such an effect, known as a marine reservoir effect (MRE), can result in radiocarbon dates from marine shells which are several hundreds of years older than coeval terrestrial organic materials (e.g., Ascough et al., 2007, 2009). The magnitude of local MREs is typically expressed as ΔR, representing the difference between a local MRE and the modelled marine calibration curve (Stuiver et al., 1986; Stuiver and Braziunas, 1993). The establishment of reliable

* Corresponding author. Departamento de Ciencias Humanas, Universidad de La Rioja, Edificio Vives, C/ Luis de Ulloa, 2, 26004, Logroño, Spain
** Corresponding author. Department of Archaeology, Max Planck Institute for the Science of Human History, Kahlaische Str. 10, 07745, Jena, Germany.
E-mail addresses: a.garcia.escarzaga@gmail.es (A. García-Escárzaga), fernandes@shh.mpg.de (R. Fernandes).

https://doi.org/10.1016/j.quageo.2021.101232
Received 28 February 2021; Received in revised form 10 September 2021; Accepted 13 September 2021
Available online 15 September 2021

chronologies for an archaeological site requires the application of corrections to marine radiocarbon dates which may, in turn, be based on previous radiocarbon measurements made on coeval terrestrial and marine samples from closed archaeological contexts (Ascough et al., 2017; Ortlieb et al., 2011).

Knowledge of temporal variations in local ΔR values for coastal European Atlantic waters during the Early and Middle Holocene is of great archaeological importance since the Mesolithic period (c. 11–6 ka cal BP) is characterized by a significant human reliance on marine resources, made visible through the large numbers of archaeological shell middens that dot the Atlantic sea-shore (Gutiérrez-Zugasti et al., 2011; Milner et al., 2007). Predictably, radiocarbon dating of marine shells is largely employed at these sites (Astrup et al., 2020; Bicho et al., 2010; García-Escárzaga et al., 2019a; Weninger et al., 2009). Furthermore, isotopic evidence for European Atlantic sites dating to the Mesolithic has revealed that humans consumed significant amounts of aquatic protein (Arias, 2006; Fontanals-Coll et al., 2014; Guiry et al., 2015; Schulting and Richards, 2001). In these cases, radiocarbon dated human remains may exhibit marine dietary radiocarbon reservoir effects (Fernandes et al., 2012, 2016; Yoneda et al., 2002). In spite of the importance of quantifying local ΔRs for archaeological research, the amount of data currently available for the European coastline during the Early Holocene remains limited. Only two previous studies have determined temporal variations in ΔR during the Mesolithic for the northern British Islands (Ascough et al., 2007, 2017) and a single study has been carried out for northern Iberian Peninsula (Soares et al., 2016), a region that is particularly rich in shell midden deposits (Arias et al., 2015; Fano, 2019; Gutiérrez-Zugasti et al., 2011). In addition to limitations in available data, recently, new calibration curves were published which require a revision of ΔR values (Heaton et al., 2020; Reimer et al., 2020).

The values of ΔR may differ for aquatic species within both marine and freshwater contexts (e.g., Forman and Polyak, 1997; Mangerud et al., 2006; Fernandes et al., 2012; 2015; England et al., 2012; Keaveney and Reimer, 2012). Such differences may arise from differences in feeding habits or spatial feeding ranges across species and from variations in ΔR during the lifetime of each species. The main source of carbon for precipitated calcium carbonate in mollusc shells is water dissolved inorganic carbon (DIC), although some lower contributions may come from metabolic carbon. This varies according to the feeding habits of different species, their metabolic system, and growth stage (Lartaud et al., 2010; Lorrain et al., 2004; Fernandes and Dreves, 2017). Significant differences may arise in ΔR values among mollusc species or between these and those of other aquatic species depending on the amount of metabolic carbon incorporated into shell carbonate and the difference between the radiocarbon concentrations of DIC and those of ingested carbon sources. Ingested carbon may also include calcareous sediments, which has been observed to result in large differences in ΔRs between deposit feeders and suspension feeders (England et al., 2012; Ferguson et al., 2011). Previous research on *Patella vulgata* from the North Atlantic showed that its ΔR did not differ significantly from four other mollusc species (*Mytilus edulis*, *Cerastoderma edule*, *Ensis ensis*, and *Littorina littorea*) (Ascough et al., 2005). Russell et al. (2011) observed different trends for ΔR in Atlantic cod (*Gadus morhua*) and *P. vulgata* although the differences were not statistically significant. Ferguson et al. (2011) found differences in ΔR between *Patella* spp. and *Mytilus galloprovincialis* shells as a result of the different feeding strategies of the two taxa. The variability in ΔR differences among mollusc species and locations described in the aforementioned studies is possibly also related to local variations in the radiocarbon concentrations of shell carbon sources. Thus, there is a need to extend the number of studies comparing ΔRs for different species and across a variety of feeding contexts.

Ideally local ΔRs would be determined at a high temporal resolution given that significant variations in local MREs may occur within short time periods (Butler et al., 2009). In practice, ΔR is often determined as a mean for a δt time interval of potentially unknown length when employing paired terrestrial and aquatic samples. An archaeological assessment is first made to establish if an archaeological context (e.g., stratum) is closed, relatively short-lived, and contains associated terrestrial and aquatic datable materials (e.g., Ascough et al., 2007, 2009). Frequently, only a single pair of terrestrial and marine samples is radiocarbon dated although multi-paired studies have shown that wide distributions may be observed for ΔR (δt) (Ascough et al., 2009; Cook et al., 2015). This variability results from the uncertainties in radiocarbon measurements, the duration of the archaeological context containing the samples, and potential age bias in archaeological samples (e.g., old wood effect for charcoal samples, collagen residence times for bone samples, species specific MREs, shape of radiocarbon calibration curve). A chi-squared test may be applied to strictly test the homogeneity of either terrestrial or aquatic samples from an archaeological context (Ward and Wilson, 1978). Samples passing the chi-squared test are often referred to as contemporaneous although such an assessment depends on the uncertainty of radiocarbon measurements which, for ^{14}C-AMS measurements of Holocene samples, is c. 30 ^{14}C years. Furthermore, different sub-groups of samples may equally pass a chi-square test without clear archaeological evidence of which sub-group to select (Scott et al., 2007). This may also be the result of an occupation length of the archaeological context beyond that assessed under the radiocarbon measurement uncertainty. By employing a sufficiently large number of measurements, depending on duration of occupation, one could characterize the distribution of different combinations of paired terrestrial and aquatic samples and summarize this as a mean and standard deviation when a normal distribution is observed. However, in practice this may not always be possible. For instance, the number of available terrestrial or aquatic suitable samples may be too low due to poor preservation.

The use of Bayesian chronological models has now become widely embraced within archaeological research (Bayliss, 2009; Hamilton and Krus, 2018). At its core is the possibility of integrating prior chronological information leading to the definition of models that combine radiocarbon measurements with other dating information such as the observable stratigraphic relationships at an archaeological site (Buck et al., 1991). The inclusion of stratigraphic information often improves the precision of individual radiocarbon measurements (Bronk Ramsey, 2009a). However, Bayesian modelling also allows for estimates of other chronological determinations such as the duration (δt) of an archaeological phase. This is particularly relevant within MRE studies given that variations in ΔR become more likely for wider time periods. Furthermore, it offers methods to detect outliers and downweigh their importance in modelling results within the temporal length of an archaeological phase (Bronk Ramsey, 2009b). In this study, we employ a Bayesian outlier model to investigate variations in ΔR (δt) across the Early and Middle Holocene at the shell midden site of El Mazo cave (Asturias, N Spain) for two of the most exploited marine mollusc species (*Patella vulgata* and *Phorcus lineatus*) by Mesolithic humans (García-Escárzaga, 2020; Gutiérrez-Zugasti et al., 2018b). To further investigate potential differences in radiocarbon contents for coeval samples of *P. vulgata* and *P. lineatus* samples we measured ^{14}C values in modern specimens from northern Spain. We also employed IRMS stable carbon isotope measurements for a selection of archaeological and modern samples to assess the carbon contributions from metabolic carbon and water DIC towards shell carbonate.

2. Background

2.1. Study area: Langre beach and shell midden site of El Mazo cave

The coastal Cantabrian region of northern Spain (Fig. 1a) is characterized by oceanic, humid and temperate climatic conditions, and has four well-differentiated seasons. The Cantabrian Sea (southern areas of the Bay of Biscay) constitutes a boundary between subtropical and boreal conditions in the Eastern Atlantic. Sea surface temperatures in the area follow a seasonal warming and cooling pattern, ranging from c. 11

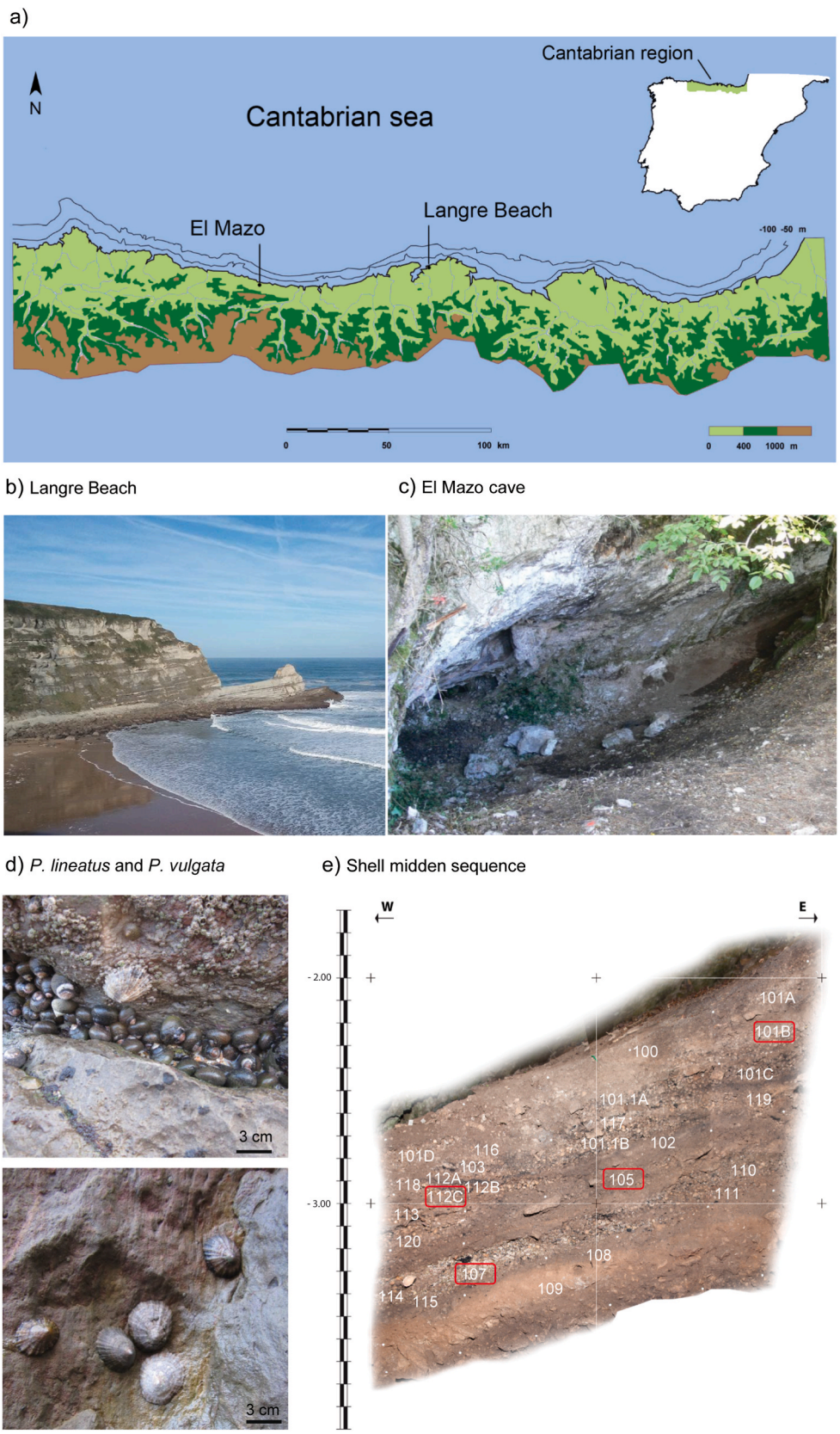

Fig. 1. Location of the a) study area (Cantabrian region) in northern Spain, b) Langre Beach and c) El Mazo Cave. d) Modern shells of *Patella vulgata* and *Phorcus lineatus* collected alive in northern Spain. e) Stratigraphy of the inner test pit (squares X15 and X16). Shell samples used in this study come from the units indicated by red rectangles.

to 23 °C during the period considered in this study (García-Escárzaga et al., 2019b; Gutiérrez-Zugasti et al., 2015, 2017). Modern shells subject to radiocarbon and stable carbon isotope measurements in this study were collected at Langre Beach (Fig. 1b) (43° 28′ 37″ N, 3° 41′ 44″ W). Previous research conducted at this site showed that sea surface salinity and oxygen isotope composition of seawater were typically marine, with some non-seasonal yearly variability and a low influence from meteoric water during the spring season (Gutiérrez-Zugasti et al., 2015, 2017). The site is not currently impacted by freshwater runoff.

The sub-fossil shells employed in our study were recovered from the Mesolithic shell midden site of El Mazo cave (Fig. 1c) (43° 24′ 04″ N, 4° 42′ 22″ W). The excavation of a test pit close to the walls of the rock shelter revealed several stratigraphic units composed of shell midden deposits, including human-made artefacts, remains of subsistence activities and other archaeological features, such as hearths. Individual shell midden units were defined by their micro- and macro-stratigraphic characteristics. Most of the units were dominated by the presence of shell remains, while some of these wire firplaces containing not only shells but also ashes and charcoal. To establish the chronology of the site, an extensive radiocarbon dating programme was developed. The radiocarbon dates published so far have placed the formation of the shell midden during the first millennia of the Holocene period, between c. 9000 and 7500 cal BP (Supplementary Material Table 1) (García-Escárzaga, 2020; García-Escárzaga et al., 2015, 2017, 2019a; Gutiérrez-Zugasti and González-Morales, 2013; Gutiérrez-Zugasti et al., 2013, 2018b; Soares et al., 2016).

2.2. Biology and ecology of Phorcus lineatus and Patella vulgata

The topshell *P. lineatus* and limpet *P. vulgata* (Fig. 1d) are marine, short-lived gastropod species that inhabit intertidal rocky shores (Crothers, 2001; Blackmore, 1969). Their geographical distribution ranges from southern Morocco to southern Britain and Ireland for *P. lineatus* (Donald et al., 2012; Kendall, 1987) and from southern Portugal to Norway for *P. vulgata* (Poppe and Goto, 1991). The spatial mobility of these two taxa seems to be limited (generally lower than 1 m per tidal cycle) and they show a marked homing behaviour, i.e., they tend to return, whenever displaced, to their original habitat zones (Díez-Urrutia, 2014; Little et al., 1988). Although the longevity of *P. lineatus* and *P. vulgata* can be up to 10 and 16 years, respectively (Crothers, 1994; Fischer-Piette, 1941), current populations rarely exceed three years in the Cantabrian region (García-Escárzaga et al., 2019b; Gutiérrez-Zugasti et al., 2015, 2017).

3. Material and methods

3.1. Modern and archaeological sample collection

Four modern specimens subject to radiocarbon measurements in this study (two *P. lineatus* and two *P. vulgata*) were collected from the intertidal rocky shore of Langre Beach (Fig. 1b) on October 1, 2012 as part of a time-extended collection programme for sclerochronological analyses of different mollusc shell species (Table 1) (Gutiérrez-Zugasti et al., 2015, 2017; García-Escárzaga et al., 2019b). The specimens were sacrificed immediately after collection by immersion in boiling water, thus avoiding further deposition of calcium carbonate. For radiocarbon and stable carbon isotope analysis a sample close to the shell edge, representative of the last portion of growth, was taken. This ensures that our comparison was on coeval materials.

A total of 31 archaeological shells were recovered from four different stratigraphic units (SUs) located within the excavation squares X15 and X16 of the shell midden site of El Mazo: SUs 107, 105, 112C and 101B (Fig. 1e). A total of 21 *P. lineatus* and four *P. vulgata* shells from units 107, 105, 112C and 101B were selected to carry out this study with a variable number of *P. lineatus* per unit and one *P. vulgata* specimen per unit (Table 2). Previous sclerochronological investigations conducted on the same modern and ancient shells studied herein, through a combination of stable oxygen isotope analyses and the study of shell growth patterns, have shown that the age of these specimens rarely exceeds three years (Gutiérrez-Zugasti et al., 2015, 2017; García-Escárzaga, 2020; García-Escárzaga et al., 2019a, 2019b). To estimate the ΔR for each stratigraphic unit a total of six terrestrial samples were taken (Table 2). These consisted of remains of charcoal from different tree species (two *Corylus avellana* and one *Quercus* sp.) and three ungulate bones (two *Capreolus capreolus* and one middle size ungulate not classified at genus level).

3.2. Methods

3.2.1. AMS radiocarbon measurements

Accelerator mass spectrometry (AMS) radiocarbon measurements were performed on previously described modern and archaeological samples. Twenty-seven out of a total of 31 archaeological samples were run at the Oxford Radiocarbon Accelerator Unit (ORAU) (Oxford, UK). Four additional subfossil shells of *P. lineatus* were run at the International Chemical Analyses (ICA) radiocarbon dating laboratory (Sunrise, USA). In both cases, standard pretreatment and routine dating procedures for marine shells and terrestrial charcoal and bones were followed (Brock et al., 2010). Radiocarbon measurements on four modern shells were undertaken at the Leibniz Laboratory for Radiometric Dating and Isotope Research (Kiel, Germany). Briefly, samples were mechanically cleaned of any adhering surface deposits and placed in a H_2O_2 solution, carbonate CO_2 was released by reacting the samples with 100% phosphoric acid, this was collected and reduced to graphite for AMS measurement (further details on measurement protocols can be found in Fernandes et al., 2012). Corrections for isotopic fractionation were done using $^{13}C/^{12}C$ ratios obtained from the AMS system at the ICA lab and measured by isotope ratio mass spectrometry (IRMS) at the ORAU lab (Stuiver and Polach, 1977). The ^{14}C concentration of a sample is expressed as percentage of modern carbon (pMC).

3.2.2. Stable carbon isotope analyses using IRMS

Stable carbon isotope ratios were measured on both modern and archaeological mollusc shells. In the case of those subfossil shells radiocarbon dated at ORAU, the pretreatment procedure developed by Brock et al. (2010) was followed and stable carbon isotope ratios were measured using IRMS methods. Stable carbon isotope ratios from modern *P. lineatus* samples were measured using an IRMS Thermo Scientific MAT 253 coupled to a Kiel IV device at the Complutense University of Madrid (Madrid, Spain). Results were compared to reference carbon dioxide obtained from the calcite international standards NBS-18 and NBS-19. Stable carbon isotope ratios from modern *P. vulgata* were measured using a Thermo Gas Bench 2 preparation system coupled to a Thermo Delta V Advantage stable-isotope ratio mass spectrometer in the

Table 1
Modern shells collected radiocarbon dated in this study and pMC values obtained from every sample.

Site	Collection date	Species description	Sample ID	Laboratory code	pMC	$\delta^{13}C$ (VPDB ‰)
Langre	October 01, 2012	*Phorcus lineatus*	Lano-5	KIA-54160	104.22 ± 0.31	0.06
	October 01, 2012	*Phorcus lineatus*	Lano-52	KIA-54161	104.14 ± 0.34	0.15
	October 01, 2012	*Patella vulgata*	Lan-25	KIA-54162	104.67 ± 0.34	−1.98
	October 01, 2012	*Patella vulgata*	Lan-29	KIA-54163	104.81 ± 0.32	−0.07

Table 2
Summary description of archaeological samples and radiocarbon and carbon stable isotope results.

Stratigraphic Unit (SU)	Square and subsquare	Spit	Material	Species description	Laboratory code	^{14}C yrs BP	pMC	δ^{13}C (VPDB ‰)	Reference
101B	X15 - C	2	Bone	*C. capreolus*	OxA-30780	7105 ± 40	41.293 ± 0.21	−22.14	Soares et al. (2016)
	X15 - C	2	Shell	*P. lineatus*	OxA-30806	7310 ± 40	40.245 ± 0.20	1.62	Unpublished data
	X15 - D	2	Shell	*P. lineatus*	OxA-33171	7475 ± 40	39.434 ± 0.20	1.20	García-Escárzaga (2020)
	X15 - D	2	Shell	*P. lineatus*	OxA-33172	7570 ± 40	38.971 ± 0.20	1.33	García-Escárzaga (2020)
	X15 - D	2	Shell	*P. lineatus*	ICA-19S/0178	7730 ± 40			Unpublished data
	X15 - D	2	Shell	*P. vulgata*	OxA-34390	7786 ± 39	37.937 ± 0.19	1.35	García-Escárzaga (2020)
112C	X16 - D	–	Bone	*C. capreolus*	OxA-28685	7367 ± 35	39.967 ± 0.18	−21.97	Unpublished data
	X16 - D	–	Shell	*P. lineatus*	OxA-28402	7425 ± 34	39.68 ± 0.17	1.17	Unpublished data
	X16 - D	–	Shell	*P. lineatus*	OxA-33173	7480 ± 40	39.406 ± 0.20	1.56	García-Escárzaga et al. (2019a)
	X16 - D	–	Shell	*P. lineatus*	OxA-33174	7565 ± 60	39.003 ± 0.30	0.9	García-Escárzaga (2020)
	X16 - D	–	Shell	*P. lineatus*	ICA-19S/0181	7720 ± 40			Unpublished data
	X16 - C	–	Shell	*P. vulgata*	OxA-34391	7733 ± 38	37.996 ± 0.18	−0.33	García-Escárzaga (2020)
105	X15 - D	2	Charcoal	*C. avellana*	OxA-30535	7380 ± 55	39.914 ± 0.27	−25.61	Soares et al. (2016)
	X16 - D	3	Shell	*P. lineatus*	OxA-33175	7530 ± 45	39.164 ± 0.21	1.04	García-Escárzaga (2020)
	X15 - D	1	Shell	*P. lineatus*	OxA-30808	7540 ± 40	39.115 ± 0.20	0.45	Unpublished data
	X16 - D	3	Shell	*P. lineatus*	OxA-33176	7580 ± 40	38.912 ± 0.20	1.58	García-Escárzaga (2020)
	X15 - D	2	Shell	*P. lineatus*	OxA-30977	7595 ± 40	38.848 ± 0.20	1.23	Soares et al. (2016)
	X16 - C	1	Shell	*P. lineatus*	OxA-28406	7566 ± 34	38.988 ± 0.17	1.11	Unpublish data
	X15 - C	3	Shell	*P. vulgata*	OxA-34392	7609 ± 39	38.78 ± 0.19	−0.82	García-Escárzaga (2020)
	X16 - D	3	Shell	*P. lineatus*	OxA-30848	7785 ± 40	37.936 ± 0.19	1.9	Unpublished data
	X15 - D	1	Shell	*P. lineatus*	OxA-28392	7926 ± 36	37.28 ± 0.17	0.8	Unpublished data
	X16 - D	3	Shell	*P. lineatus*	ICA-19S/0179	7980 ± 40			Unpublished data
107	X15 - C	3	Charcoal	*C. avellana*	OxA-28395	7438 ± 35	39.617 ± 0.18	−25.4	Unpublished data
	X16 - D	1	Charcoal	*Quercus*	OxA-28407	7694 ± 36	38.375 ± 0.17	−24.36	Unpublished data
	X16 - D	1	Bone	Middle size ungulate	OxA-28408	7618 ± 37	38.737 ± 0.18	−18.51	Unpublished data
	X16 - D	1	Shell	*P. lineatus*	OxA-28409	7681 ± 34	38.436 ± 0.16	1.72	Unpublished data
	X16 - D	1	Shell	*P. lineatus*	OxA-33178	7730 ± 40	38.2 ± 0.19	1.68	García-Escárzaga (2020)
	X16 - D	1	Shell	*P. lineatus*	OxA-33177	7805 ± 40	37.837 ± 0.20	0.8	García-Escárzaga (2020)
	X16 - D	1	Shell	*P. lineatus*	ICA-19S/0180	7870 ± 40			Unpublished data
	X16 - C	1	Shell	*P. lineatus*	OxA-28410	7929 ± 35	37.268 ± 0.16	0.08	Unpublished data
	X16 - D	1	Shell	*P. vulgata*	OxA-34502	7935 ± 38	37.238 ± 0.18	−1.14	García-Escárzaga (2020)

Stable Isotope Facility at the University of Bradford (Bradford, UK). Standardisation of measured values was undertaken using repeated measurements of international standards NBS-19 and IAEA–CO–1. All results are expressed using delta notation (δ^{13}C) relative to the calcite international standard Vienna Pee Dee Belemnite (VPDB). The analytical error based on repeat measurement of an in-house MERCK carbonate standard was better than ±0.1‰ for Complutense University of Madrid and University of Bradford laboratories. For specimens ^{14}C measured at ICA, δ^{13}C data is not available.

3.2.3. Bayesian chronological modelling

Bayesian chronological modelling was performed using the software package OxCal v. 4.4 (Bronk Ramsey, 2009a) and the IntCal20 and Marine20 calibration curves for terrestrial and marine samples, respectively (Heaton et al., 2020; Reimer et al., 2020) (Supplementary Material Code 1). Samples from each stratigraphic unit were grouped as Phases separated by Boundaries using OxCal terminology. We did not assume that adjacent stratigraphic units shared a common boundary allowing for a temporal gap between the end of a phase and the start of

an adjacent one. We employed an outlier general model to detect the possible intrusion of samples into a stratigraphic layer that did not belong to the original deposition (Bronk Ramsey, 2009b). We assumed that temporal outliers followed a Student's t distribution with 5 degrees of freedom, and we employed a wide scale (0–10,000 years). To each sample, a prior probability of 5% that it was an outlier was assigned. The different phases were distributed according to their stratigraphic sequence using the Sequence function (OxCal terminology). Mollusc samples were assigned a wide uniform ΔR prior between −800 and 800 years. Estimates for mean ΔR according to each species and phase (duration, start, and end) are expressed as 68% and 95% credible intervals corresponding to the highest probability densities. To obtain average ΔR estimates across multiple stratigraphic units and for both mollusc species we summed the posterior distributions for individual stratigraphic units and species using the OxCal function "Sum".

3.2.4. Bayesian mixing modelling

The ReSources open access software, developed within the Pandora & IsoMemo initiatives (https://isomemoapp.com), was employed to estimate the carbon contribution from different sources (water DIC, metabolic limestone carbonate, and metabolic organics) towards mollusc shell. A concentration-independent model was undertaken following the same specification described for the FRUITS software package (Fernandes et al., 2014). As an isotopic proxy for source carbon contributions, we employed the stable carbon isotope measurements on mollusc shells and carbon sources. As reference source isotopic values, we took the mid-point and range of previously reported $\delta^{13}C$ ranges for red algae (−27.2 ± 10.5‰) and green algae (−13.6 ± 3.2‰) collected off the coast of Brittany in France (Adin and Riera, 2003), carbonate limestone (1.7 ± 1.6‰) from coastal Basque Country in Spain (Perona et al., 2018), and marine water DIC (−3.9 ± 2.4‰) from the Cantabrian region in Spain (Milano et al., 2020). We employed a random effects structure on the categorical covariate "Species" with two levels corresponding to specimens from each mollusc species. In contrast to a model without covariates, the Dirichlet prior values of the source contribution parameters are not fixed but come from a distribution with common mean and standard deviation for each factor level and source group.

As modelled prior information, it was assumed that the major carbon source was DIC, followed by organic carbon, and finally limestone. There is no well-defined isotopic offset for inorganic and metabolic contributions toward shell $\delta^{13}C$ carbonate for the mollusc species in this study. Several complications arise when determining this, water DIC measurements primarily reflect bicarbonate for standard marine pH ranges (the other carbon molecular species are carbon dioxide and carbonate) although carbon dioxide seems to be the major contributor for biological calcification (McConnaughey and Gillikin, 2008; Solomon et al., 2006). A full model accounting for full isotopic fractionation would have to consider the fractionation between ambient DIC or diet and blood DIC plus the fractionation between the calcification site and blood (McConnaughey and Gillikin, 2008; Solomon et al., 2006). In addition, experiments using synthetic aragonite and calcite showed a small difference in isotopic fractionation during inorganic precipitation (Romanek et al., 1992). In spite of all of these complications, the net fractionation effect seems to be small and shell $\delta^{13}C$ is usually a few ‰ smaller than water DIC, similar to what has been observed for fish otoliths (McConnaughey and Gillikin, 2008; Solomon et al., 2006). The latter was quantified as −2.7‰±1.2‰ but here we employed a more conservative range (−2.7‰±3‰) (Solomon et al., 2006). The posterior distributions for estimated carbon contributions are summarized as credible intervals (68% and 95%) with the distributions for red and green algae added and summarized as an organic contribution.

4. Results and discussion

4.1. Radiocarbon and $\delta^{13}C$ differences in modern and past P. lineatus and P. vulgata

To assess potential ^{14}C differences between *P. lineatus* and *P. vulgata* we relied on radiocarbon measurements on modern coeval samples. Sclerochronological analyses conducted on four modern shells showed that the shell portions taken for measurement were synthesised during the last months prior to mollusc collection (Gutiérrez-Zugasti et al., 2015, 2017) that is, from July to September 2012. The mean radiocarbon activity results for modern *P. lineatus* and *P. vulgata* were 104.18 ± 0.23 pMC and 104.74 ± 0.24 pMC (Table 1), respectively. These values are slightly higher than the mean radiocarbon activity observed during July–September 2012 for atmospheric CO_2 (103.8 ± 0.02 pMC) (Hammer and Levin, 2017). Atmospheric ^{14}C activity had a steep rise after 1950 as a result of atmospheric nuclear weapon tests, reaching a peak in 1963 and has become smaller, albeit with some oscillations, since then. Under a MRE of c. 400 years (marine global average) values of c. 99 to 100 pMC would be expected for the molluscs at Langre beach. Although local MREs are expected to differ from the marine global average, the ^{14}C difference between mollusc shell and contemporary atmospheric CO_2 is considerably smaller than expected and suggests the local presence of ^{14}C-enriched carbon pools.

The difference between the mean ^{14}C activities for the two modern mollusc species (0.56 pMC) is significant at the 1-sigma level and equivalent to c. 45 ^{14}C years during the Holocene, with *P. vulgata* showing a higher concentration than *P. lineatus*. In comparison, the ΔR 68% credible intervals for archaeological samples show only minor overlaps between the two species, particularly for unit 105, although there are considerable overlaps for the 95% credible intervals (Table 3; Fig. 2). In this case, the results indicate that *P. lineatus* has a higher ^{14}C content than *P. vulgata* (Table 2). The average difference between the species across archaeological contexts is 142 ± 150 ^{14}C years. Higher metabolic contribution towards mollusc shell from limestone with ^{14}C activity ≈0 for *P. vulgata* would provide a justification as to why its respective archaeological shells have lower ^{14}C contents than those observed for *P. lineatus*. The fact that the opposite is observed in modern samples may be the result of the presence of an unusually enriched ^{14}C source or sources, including surface organic matter with a long residence time and a higher ^{14}C content due to the bomb effect. The high ^{14}C values observed in modern specimens allow for this possibility and future ^{14}C measurements on the different local carbon pools could be used to test this hypothesis.

The ^{14}C values for mollusc shells will depend on a complex combination of local mollusc feeding practices, percentage of contribution of metabolic intakes towards shell carbonate, and the ^{14}C concentration of source carbon pools (Fernandes and Dreves, 2017). In the absence of data for these variables, we defined simple simulation scenarios with variations for these (simulated values given in Table 4) to illustrate how these can result in varying differences in ^{14}C shell values for hypothetical specimens (Fig. 3a). Particularly relevant to our modern vs. past mollusc measurement comparison are the simulated results for scenarios 1 and 2 that show how differences in ^{14}C shell among specimens can diverge, and even invert the sign of their different, with variations in ^{14}C values for source organic and DIC carbon pools provided that the amounts at which these contribute to shell carbon vary with specimen. Scenarios 3 and 4 illustrate how differences in ^{14}C shell among specimens can quickly increase with larger contributions from limestone for one of the specimens, reaching as high as several hundred years (for Holocene samples 1 pMC ≈80 ^{14}C years). A previous study by Ferguson et al. (2011) revealed ^{14}C differences between limpets and mussels of up to c. 1500 ^{14}C years. While other studies show a variety of magnitudes for ^{14}C differences or their absence (Ascough et al., 2005; Russell et al., 2011), including a study on limpets from regions with a carbonate geology that revealed no significant shell ^{14}C depletion (Allen et al., 2019).

Table 3
Marine reservoir effect diachronic results for northern Spain obtained for *Phorcus lineatus* and *Patella vulgata* shell species recovered from El Mazo cave. Species-specific ΔR values (Supplementary Material Figs. 1–8), as well as ΔR mean values for both species are reported for each stratigraphic unit. ΔR values and ΔR weighted mean values for all stratigraphic units and for all stratigraphic units excluding unit 101B are also reported. ΔR weighted mean estimates are only available when the combined individual results passed a χ^2-Test (Supplementary Material Text 1).

Stratigraphic Unit 101B (c. 7.9 ka cal BP)

	68% credibility interval		95% credibility interval		μ	σ	m
	From	To	From	To			
P. vulgata	−24	194	−125	349	102	119	91
P. lineatus	−208	−19	−294	110	−98	104	−107
Mean	−173	130	−270	291	**2**	**150**	−8

Stratigraphic Unit 112C (c. 8.1 ka cal BP)

	68% credibility interval		95% credibility interval		μ	σ	m
	From	To	From	To			
P. vulgata	−205	−29	−301	59	−117	92	−116
P. lineatus	−352	−224	−430	−173	−293	66	−290
Mean	−341	−83	−416	24	**−205**	**119**	−222

Stratigraphic Unit 105 (c. 8.2 ka cal BP)

	68% credibility interval		95% credibility interval		μ	σ	m
	From	To	From	To			
P. vulgata	−370	−192	−464	−93	−278	94	−280
P. lineatus	−408	−288	−453	−213	−339	61	−344
Mean	−403	−245	−464	−128	**−309**	**85**	−318

Stratigraphic Unit 107 (c. 8.4 ka cal BP)

	68% credibility interval		95% credibility interval		μ	σ	m
	From	To	From	To			
P. vulgata	−254	−75	−341	19	−163	90	−165
P. lineatus	−352	−240	−414	−184	−298	56	−298
Mean	−352	−147	−408	−19	**−231**	**101**	−246

All stratigraphic units

	68% credibility interval		95% credibility interval		μ	σ	m	ΔR weighted mean value
	From	To	From	To				
P. vulgata	−322	8	−419	237	**−114**	**170**	−134	**−134 ± 49**
P. lineatus	−400	−208	−448	8	**−257**	**120**	−283	**−288 ± 34**
Both species	−384	−82	−445	173	**−186**	**163**	−221	**Failed χ^2-test**

Stratigraphic units 107 – 105 – 112C

	68% credibility interval		95% credibility interval		μ	σ	m	ΔR weighted mean value
	From	To	From	To				
P. vulgata	−296	−64	−418	30	**−186**	**115**	−182	**−184 ± 54**
P. lineatus	−376	−243	−435	−189	**−310**	**65**	−309	**−310 ± 35**
Both species	−387	−173	−440	−14	**−248**	**112**	−266	**−238 ± 28**

To assess potential differences in the contributions from source carbon pools towards the shell carbonate of *P. lineatus* and *P. vulgata* we relied on Bayesian mixing modelling of stable carbon isotope data. The modelling results show that there can be important contributions from organic carbon to shell carbonate and a small (near zero) contribution from limestone (Fig. 3b). The estimated mean contribution from organics towards shell carbonates is c. 10% for *P. lineatus* and c. 20% for *P. vulgata* which is consistent with previously reported estimates which are often above 10% (McConnaughey and Gillikin, 2008). The overlap in credible intervals for both species does not allow for a clear differentiation of their respective shell carbon sources although the mean contribution from DIC toward *P. lineatus* shell is lower than that for *P. vulgata* with the latter having higher mean values for the carbon contributions from organics and limestone. Both species are microphagous herbivores that feed on microscopic plants, especially diatoms, by grazing the rocky substrate using their corneous tongue (radula) (Crothers, 2001, 2003; Hawkins et al., 1989; Sousa et al., 2018). A recent study has shown that limpet teeth represent the strongest natural material (Barber et al., 2015) and *P. vulgata* has harder teeth than *P. lineatus* (Barber et al., 2015; Hawkins et al., 1989; Crothers, 2001). *P. vulgata* has been shown to consume higher amounts of surface deposits as evidenced by deeper marks left on rock surfaces (Crothers, 2001, 2003). Thus, we considered an additional Bayesian mixing model with the added prior that the carbon contributions from limestone to shell carbonate for *P. vulgata* was higher than that for *P. lineatus*. This led to an overall increase in estimate precision (Fig. 3b). Estimate means for limestone carbon contributions suggest that these are ~2% higher for *P. vulgata* which, under conditions where near surface marine DIC and organics ^{14}C values do not differ greatly (similar to simulated scenario 3), lead to a difference in ΔR values between species of ~160 ^{14}C years which is similar to the observed archaeological mean difference (142 ± 150 ^{14}C years). For this offset to be reversed (i.e., *P. vulgata* with a higher ^{14}C content than *P. lineatus*), as observed in modern molluscs, would require that the contribution from organics to the shell carbonate is higher for *P. vulgata* than *P. lineatus* (difference in Bayesian estimate means show this to be ~15% higher) and that organic carbon sources have a higher ^{14}C content than DIC (similar to simulated scenario 2), as discussed previously.

4.2. Radiocarbon chronology of archaeological contexts

The Bayesian chronological model showed 7 samples with posterior probabilities greater than 5% (up to 34%, Supplementary Data 1). With two outliers (OxA-28392 and ICA-19S/0179I) from the stratigraphic

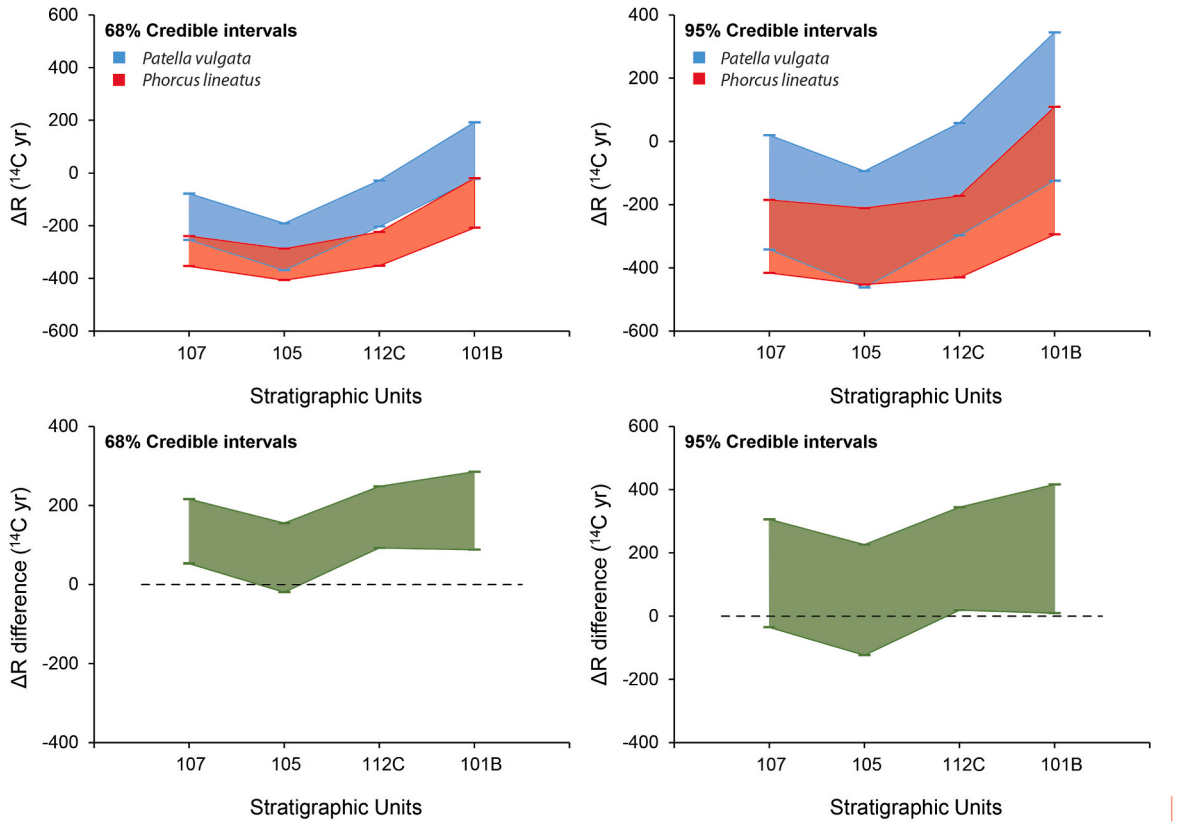

Fig. 2. Credibility intervals for Bayesian estimates of ΔR for archaeological *P. vulgata* and *P. lineatus* and for the difference among these.

Table 4
Settings for variables defined across four different scenarios to simulate ^{14}C values in carbonate from mollusc shells.

		^{14}C DIC (pMC)	^{14}C Limestone (pMC)	^{14}C Organics (pMC)	% DIC	% Limestone	% Organics
Scenario 1	Specimen 1	Variable	0	80	65	10	25
	Specimen 2	Variable	0	80	70	10	20
	Specimen 3	Variable	0	80	60	10	30
Scenario 2	Specimen 1	100	0	Variable	65	10	25
	Specimen 2	100	0	Variable	70	10	20
	Specimen 3	100	0	Variable	60	10	30
Scenario 3	Specimen 1	95	0	80	65	10	25
	Specimen 2	95	0	80	70	Variable	Variable
	Specimen 3	95	0	80	60	Variable	Variable
Scenario 4	Specimen 1	100	0	105	65	10	25
	Specimen 2	100	0	105	70	Variable	Variable
	Specimen 3	100	0	105	60	Variable	Variable

unit SU 105 having near 100% posterior outlier probabilities and a negligible weight in modelling results. The formation of the four stratigraphic units took place between c. 8.6 ka and 7.5 ka cal BP (Fig. 4). Bayesian chronological estimates show that stratigraphic units 105 (c. 8.2 ka cal BP) and 112C (c. 8.1 ka cal BP) likely coincide with the 8.2 ka cal BP cold climate abrupt event (8.25–8.09 ka cal BP) (Alley et al., 1997; Thomas et al., 2007). Bayesian estimates also suggest that the duration of the different units could have differed. While SUs 107 and 101B exhibit longer durations (SU 107: between 88 and 242 years for a 68% credibility interval and between 0 and 312 years for a 95% credibility interval; SU 101B: between 0 and 206 years for a 68% credibility interval and between 0 and 445 years for a 95% credibility interval), 105 and 112C had shorter durations (SU 105 between 0 and 74 years for a 68% credibility interval and between 0 and 180 years for a 95% credibility interval; SU 112C: between 0 and 95 years for a 68% credibility interval and between 0 and 204 years for a 95% credibility interval).

4.3. ΔR variability during the mesolithic

Both *P. vulgata* and *P. lineatus* mollusc species exhibited similar trends for ΔR credible intervals throughout the shell midden stratigraphic sequence (Table 3, Fig. 2). The lowest ΔR credible intervals for both species were observed in unit 105 (*P. vulgata*: between −370 and −192 for a 68% credibility interval and between −464 and −93 for a 95% credibility interval; *P. lineatus*: between −408 and −288 for a 68% credibility interval and between −453 and −213 for a 95% credibility interval), while the largest ΔR credible intervals were observed in the most recent stratigraphic unit, i.e., 101B (*P. vulgata*: between −24 and 194 for a 68% credibility interval and between −125 and 349 for a 95% credibility interval; *P. lineatus*: between −208 and −19 for a 68% credibility interval and between −294 and 110 for a 95% credibility interval). However, the 68% credible intervals for the different layers overlap for each species with the exception of unit 112C (Fig. 2).

The relatively large credible intervals in our ΔR estimates likely arise

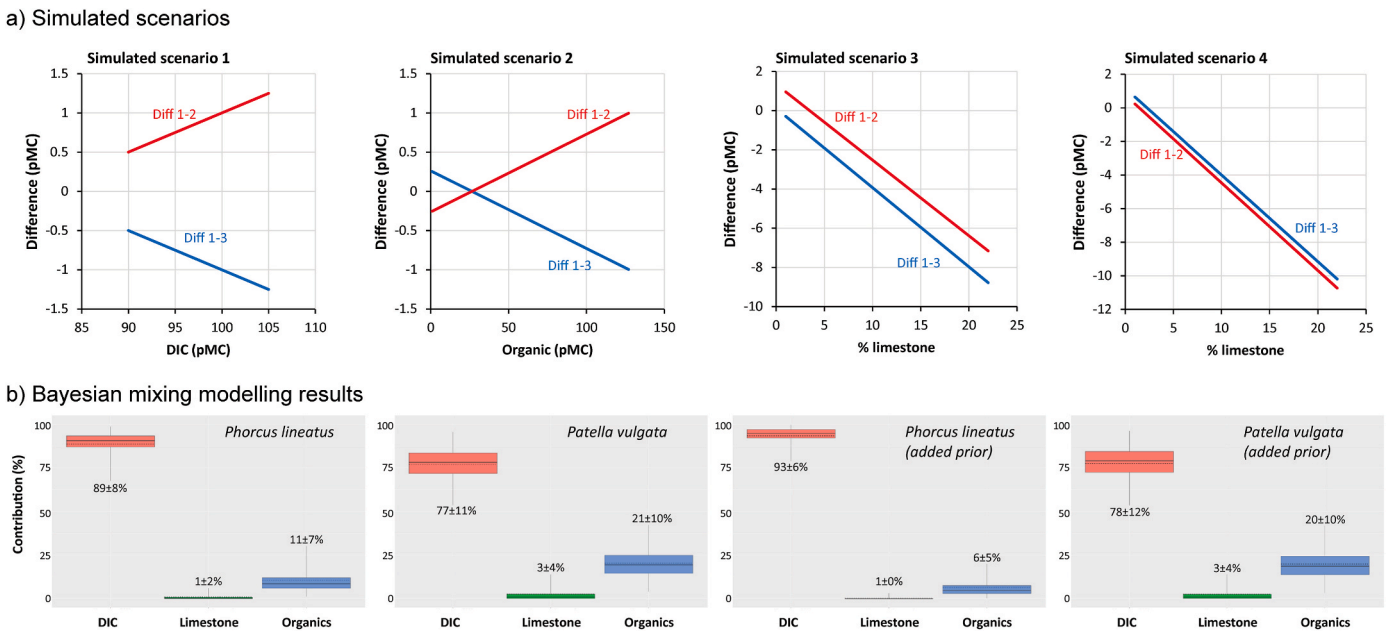

Fig. 3. a) Simulated ^{14}C differences among mollusc specimens with simulation parameters defined in Table 4 b) Bayesian estimates of carbon contributions to shells of *Phorcus lineatus* and *Patella vulgata*. Two estimates are shown. With and without an additional prior that limestone contribution to shell carbonate was larger for *Patella vulgata* than for *Phorcus lineatus*.

from our limited number of terrestrial and *P. vulgata* samples plus the likely extended temporal use of the archaeological units. Previously published radiocarbon results on paired terrestrial and marine samples, consisting of one specimen each, from northern Iberian Mesolithic contexts revealed some differences in ΔR values, although a more positive result was discarded as an outlier (Soares et al., 2016). However, current available radiocarbon dates for El Mazo cave suggest that levels could have been formed throughout several decades or even centuries (Table 2, Fig. 3) and thus terrestrial and marine samples might not be contemporaneous. The clearest examples of this are units 101B and 107 for which the modelling results allow for a potential use of up to several hundred years, as discussed previously. For unit 107, the combination of all marine samples fails to pass a χ^2-Test (all marine samples: df = 4 T = 32.0 (5% 9.5) with mean = 7803 ± 17 yrs BP) but sub-groups of measurements do pass the test with significantly different means: (OxA-33177, ICA-19S/0180, and OxA-28410: df = 2 T = 5.4 (5% 6.0) with mean = 7874 ± 22 yrs BP) versus (OxA-28409 and OxA-33178: df = 1 T = 0.9 (5% 3.8) with mean = 7702 ± 26 yrs BP). The same applies to unit 101B: (all marine samples: df = 4 T = 93.9 (5% 9.5) with mean = 7582 ± 18 yrs BP) and sub-groups (OxA-33171 and OxA-33172: df = 1 T = 2.8 (5% 3.8) with mean = 7523 ± 29 yrs BP) versus (ICA-19S/0178 and OxA-34390: df = 1 T = 1.0 (5% 3.8) with mean = 7759 ± 28 yrs BP). For unit 101B, previous studies (Soares et al., 2016) relied only on the radiocarbon measurement from shell OxA-30806 that had the lowest ^{14}C value among all shells from unit 101B (Table 1; 7310 ± 40 yrs BP). Furthermore, the terrestrial samples for layer 101B also do not pass the χ^2-Test (all terrestrial samples: df = 2 T = 27.4 (5% 6.0) with mean = 7528 ± 21 yrs BP).

Temporal variations in ΔR can arise from a variety of environmental phenomena (Alves et al., 2018; Teller et al., 2012). Upwelling, in particular, is an upward movement of deep and ^{14}C-depleted waters to shallow waters (Ascough et al., 2005; Bicho et al., 2010; Stuiver and Braziunas, 1993). A rise in the contribution of ^{14}C-depleted freshwater to marine systems could lead to an increase of marine ΔR values (Teller et al., 2012). This phenomenon was previously documented for the 8.2 ka cal BP cold event on the Portuguese coast (Bicho et al., 2010), one of the most significant climatic anomalies during the first few millennia of the Holocene (Allen et al., 2007; Thomas et al., 2007). It was characterised by overall dryer conditions and lower temperatures in the northern hemisphere, both in marine and terrestrial environments (Risebrobakken et al., 2003; Rohling and Pälike, 2005). This abrupt climate event was the result of a previous outburst of glacial meltwater ($\delta^{18}O$-depleted) from the Laurentide lakes in northern America (c. 8.5–8.3 ka cal BP) (Barber et al., 1999; Lewis et al., 2012; Lochte et al., 2019). The influx of this cold freshwater into the Atlantic Ocean led to a reduction of sea-surface salinity and a decline of the Atlantic meridional overturning circulation (AMOC), leading to a reduction of sea surface temperatures (SST) across the North Atlantic area (Alley and Ágústsdóttir, 2005; Mary et al., 2017). According to Teller et al. (2002), the massive volume of ^{14}C-depleted freshwater from ice sheets caused an increase in ΔR values in the northern Atlantic – a phenomenon that has been observed in the Portuguese coast (Bicho et al., 2010; Soares and Dias, 2006). This freshwater outburst has been detected using $\delta^{18}O$ measurements in foraminifera and speleothems throughout the North Atlantic, including northern Iberian Peninsula (Domínguez-Villar et al., 2009; Hoffman et al., 2012; Rossi et al., 2018). The 8.2 ka abrupt event also had important climatic consequences for northern Iberia (Nuñez de la Fuente, 2018; Rossi et al., 2018; Smith et al., 2016). A recent study showed a decline of littoral SST during the 8.2 ka event, reaching a minimum during the formation of unit 112C (García-Escárzaga, 2020). A rise in ΔR values for archaeological layers above unit 105 at El Mazo cave (dated to c. 8.2 ka cal BP) could have been the consequence of a freshwater outburst. The possible increase in ΔR for unit 101B (c. 7.8 ka cal BP) relative to unit 105 may also have been accentuated by local deglaciation processes occurring after the 8.2 ka event as a consequence of a rise in local temperatures (Moreno et al., 2011; García-Escárzaga, 2020).

4.4. Chronological consequences of MRE results

Our results provide updated estimates for marine radiocarbon reservoir effects in northern Iberia during the Early and Middle Holocene. These estimates are crucial for chronological corrections to radiocarbon measurements on marine shells, in particular for samples recovered from Mesolithic contexts. In addition, estimates of ΔR are also necessary for correction of radiocarbon dates on remains from past

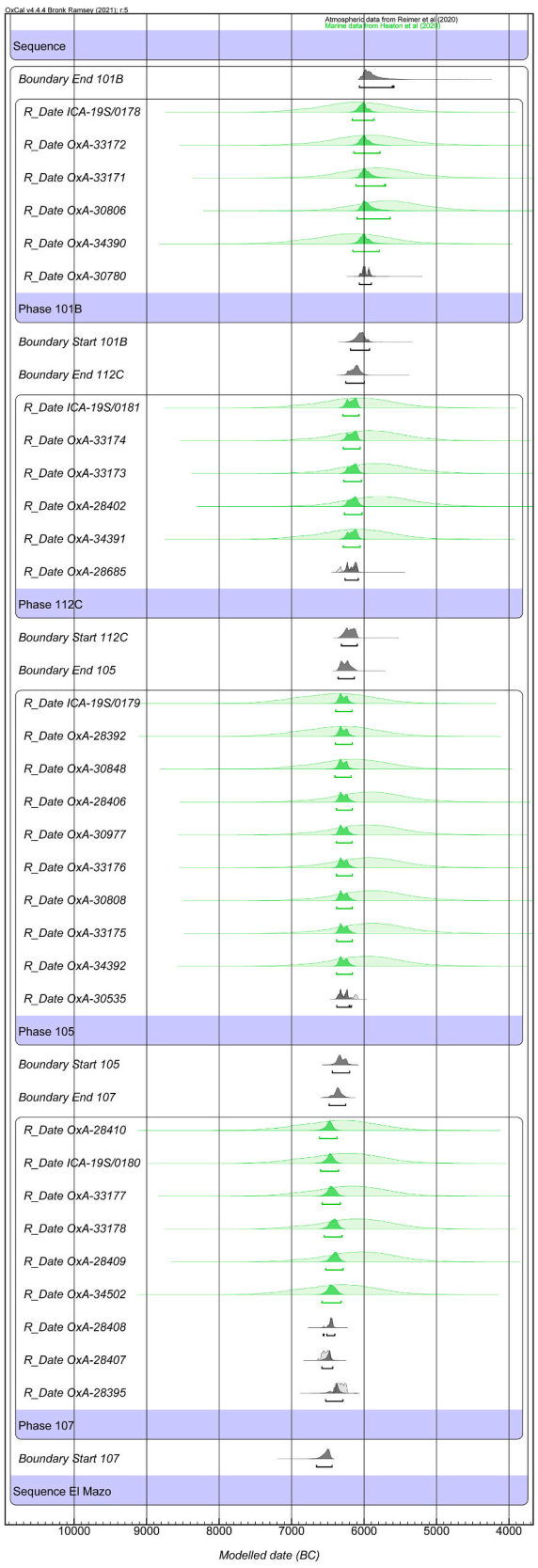

Fig. 4. Bayesian modelling results for the stratigraphic sequence at El Mazo cave. Generated using the software OxCal v. 4.4 (Bronk Ramsey, 2009a) and the calibration curves IntCal20 and Marine20 (Reimer et al., 2020; Heaton et al., 2020).

humans, and potentially other animals, that consumed marine foods (Fernandes et al., 2012, 2016; Yoneda et al., 2002). One of the most characteristic features of the Mesolithic period along Atlantic littoral is that the Mesolithic groups largely consumed marine resources (Arias, 2015; Fontanals-Coll et al., 2014; Guiry et al., 2015; Schulting and Richards, 2001).

In our modelling we produced separate ΔR estimates for *P. lineatus* and *P. vulgata*, the two mollusc species most exploited by humans during the Early and Middle Holocene in the northern Iberian Peninsula. In addition, we estimated ΔR distributions for combinations of different species and time periods (Table 3). We also calculated weighted means and standard error of the means when ΔR distributions followed approximately a Gaussian distribution and their combination passed a χ^2-Test (Supplementary Material Text 1). This leads to a comparatively low uncertainty and should be considered as a non-conservative estimate. Our recommendation is that a hierarchical approach to the selection of the appropriate ΔR distribution in future studies should be taken. Ideally, the ΔR distribution for a specific species and time period should be employed. When the former is not known (e.g., in human studies) then the ΔR distribution combining both species should be employed instead and the same principle should be followed for the chronological assignment. That is, if the marine species or human being dated cannot be placed within a certain chronological interval corresponding to the El Mazo layers then a temporal mean for multiple periods can be employed instead. The use of a weighted ΔR mean and standard error should be justified, namely by relatively similar environmental conditions that would lead to similar ΔRs. However, as discussed previously, this might not be the case at El Mazo. It is also worth noting that our study is limited to a single location and that the use of the ΔR distributions reported here may not be applicable to other regions and that it is also difficult to define a radius of applicability. Nonetheless, it does offer an updated ΔR reference for northern Iberian during the Early and Middle Holocene. In cases where future modelling applications require a single ΔR reference we propose that the value -238 ± 28 ^{14}C years is employed (more conservative approaches should use -248 ± 112 ^{14}C years) for marine samples dating to before c. 8.1 ka cal BP whereas for later samples a conservative reference value should be employed (2 ± 150 ^{14}C years).

5. Conclusions

Bayesian modelling provides a platform for the modelling of complex chronological phenomena. In this study, we established the Bayesian chronology for several units from the El Mazo site in northern Spain. According to the modelling results, the four stratigraphic units considered in this study (107, 105, 112C and 101B) were formed between c. 8.6 ka and 7.5 ka cal BP, and some could have been occupied for extended time periods. Our results suggest a pattern in temporal changes in local ΔRs and variation according to species, although estimate precision was limited. This is characterized by a stable or slightly decreasing ΔR between layers 107 and 105 followed by a steady increase until the final layer. An outburst of glacial meltwater depleted in ^{14}C (c. 8.5–8.3 ka cal BP) from the Laurentide lakes in North America likely led to the increase in ΔR during and after layer 105. This outburst is also identified as the cause for the most prominent global climate anomaly thus far identified during the Holocene, the 8.2 ka cal BP event. Deglaciation processes occurring after the 8.2 ka event could have accentuated rises in ΔR. Radiocarbon results also revealed differences in ΔR values for *P. lineatus* and *P. vulgata* although these were only significant or approximately significant at the 1-sigma level. In view of the results, we propose different reference ΔR values for chronological corrections in northern Iberia according to chronology, mollusc species, and their combination. A non-conservative ΔR reference for marine samples dating earlier than c. 8.1 ka cal BP is -238 ± 28 ^{14}C years.

Declaration of competing interest

The authors declare that they have no known competing financial interests or personal relationships that could have appeared to influence the work reported in this paper.

Acknowledgments

This research was performed as part of the projects HAR 2016-75605-R and HAR 2017-86262-P, funded by the Spanish Ministry of Economy and Competitiveness, MINECO. During the development of this research AGE was funded by the Basque Country Postdoctoral Programme through a postdoctoral grant (POS_2020_2_0032) and University of La Rioja (no code available). This study has also been supported by the Prehistoric Research Consolidated Group of the Basque Country University (IT-1223-19), funded by the Basque Country Government. PR and RF are funded by the Max Planck Society. We thank the Fishing Activity Service of the Cantabrian Government for the authorization to collect modern specimens. We also thank the Max Plank Society, University of La Rioja, Basque Country University (UPV/EHU), University of Cantabria (UC) and Instituto Internacional de Investigaciones Prehistóricas de Cantabria (IIIPC) for providing support.

Appendix A. Supplementary data

Supplementary data to this article can be found online at https://doi.org/10.1016/j.quageo.2021.101232.

References

Adin, R., Riera, P., 2003. Preferential food source utilization among stranded macroalgae by Talitrus saltator (Amphipod, Talitridae): a stable isotopes study in the northern coast of Brittany (France). Estuarine. Coastal and Shelf Science 56, 91–98.
Allen, J.R., Long, A.J., Ottley, C.J., Pearson, D.G., Huntley, B., 2007. Holocene climate variability in northernmost Europe. Quat. Sci. Rev. 26, 1432–1453.
Allen, K.R., Reimer, P.J., Beilman, D.W., Crow, S.E., 2019. An investigation into 14C offsets in modern mollusk shell and flesh from Irish coasts shows no significant differences in areas of carbonate geology. Radiocarbon 61, 1913–1922.
Alley, R.B., Ágústsdóttir, A.M., 2005. The 8k event: cause and consequences of a major Holocene abrupt climate change. Quat. Sci. Rev. 24, 1123–1149.
Alley, R.B., Mayewski, P.A., Sowers, T., Stuiver, M., Taylor, K.C., Clark, P.U., 1997. Holocene climatic instability: a prominent, widespread event 8200 yr ago. Geology 25, 483–486.
Alves, E.Q., Macario, K., Ascough, P., Bronk Ramsey, C., 2018. The worldwide marine radiocarbon reservoir effect: definitions, mechanisms, and prospects. Rev. Geophys. 56, 278–305.
Arias, P., 2006. Determinaciones de isótopos estables en restos humanos de la región Cantábrica. Aportación al estudio de la dieta de las poblaciones del Mesolítico y el Neolítico. Munibe 57, 359–374.
Arias, P., Cubas, M., Fano, M.Á., Jordá-Pardo, J.F., Salzmann, C., Teichner, F., Teira, L.C., 2015. Where are the 'Asturian'dwellings? An integrated survey programme on the Mesolithic of northern Spain. Antiquity 89 (346), 783–799.
Ascough, P.L., Cook, G.T., Dugmore, A.J., Scott, E.M., Freeman, S.P., 2005. Influence of mollusk species on marine ΔR determinations. Radiocarbon 47 (3), 433–440.
Ascough, P.L., Cook, G.T., Dugmore, A.J., Scott, E.M., 2007. The North Atlantic marine reservoir effect in the Early Holocene: implications for defining and understanding MRE values. Nucl. Instrum. Methods Phys. Res. Sect. B Beam Interact. Mater. Atoms 259 (1), 438–447.
Ascough, P.L., Cook, G.T., Dugmore, A.J., 2009. North Atlantic marine 14C reservoir effects: implications for late-Holocene chronological studies. Quat. Geochronol. 4 (3), 171–180.
Ascough, P.L., Church, M.J., Cook, G.T., 2017. Marine radiocarbon reservoir effects for the Mesolithic and Medieval periods in the western isles of Scotland. Radiocarbon 59 (1), 17–31.
Astrup, P.M., Skriver, C., Benjamin, J., Stankiewicz, F., Ward, I., McCarthy, J., Ross, P., Baggaley, P., Ulm, S., Bailey, G., 2020. Underwater shell middens: excavation and remote sensing of a submerged mesolithic site at hjarnø, Denmark. J. I. Coast Archaeol. 15, 457–476.
Barber, D.C., Dyke, A., Hillaire-Marcel, C., Jennings, A.E., Andrews, J.T., Kerwin, M.W., Bilodeau, G., McNeely, R., Southon, J., Morehead, M.D., Gagnon, J.M., 1999. Forcing of the cold event of 8,200 years ago by catastrophic drainage of Laurentide lakes. Nature 400, 344.
Barber, A.H., Lu, D., Pugno, N.M., 2015. Extreme strength observed in limpet teeth. J. R. Soc. Interface 12 (105), 20141326.
Bayliss, A., 2009. Rolling out revolution: using radiocarbon dating in archaeology. Radiocarbon 51 (1), 123–147.
Bicho, N., Umbelino, C., Detry, C., Pereira, T., 2010. The emergence of Muge Mesolithic shell middens in central Portugal and the 8200 cal yr BP cold event. J. I. Coast Archaeol. 5 (1), 86–104.
Blackmore, D.T., 1969. Studies of Patella vulgata L. I. Growth, reproduction and zonal distribution. J. Exp. Mar. Biol. Ecol. 3 (2), 200–213.
Bosch, M.D., Mannino, M.A., Prendergast, A.L., O'Connell, T.C., Demarchi, B., Taylor, S. M., Niven, L., van der Plicht, J., Hublin, J.-J., 2015. New chronology for Ksâr 'Akil (Lebanon) supports Levantine route of modern human dispersal into Europe. Proc. Natl. Acad. Sci. Unit. States Am. 112 (25), 7683–7688.
Brock, F., Higham, T., Ditchfield, P., Bronk Ramsey, C., 2010. Current pretreatment methods for AMS radiocarbon dating at the Oxford radiocarbon accelerator unit (Orau). Radiocarbon 52, 103–112.
Bronk Ramsey, C., 2009a. Bayesian analysis of radiocarbon dates. Radiocarbon 51, 337–360.
Bronk Ramsey, C., 2009b. Dealing with outliers and offsets in radiocarbon dating. Radiocarbon 51, 1023–1045.
Buck, C.E., Kenworthy, J.B., Litton, C.D., Smith, A.F., 1991. Combining archaeological and radiocarbon information: a Bayesian approach to calibration. Antiquity 65 (249), 808–821.
Butler, P.G., Scourse, J.D., Richardson, C.A., Wanamaker Jr., A.D., Bryant, C.L., Bennell, J.D., 2009. Continuous marine radiocarbon reservoir calibration and the 13C Suess effect in the Irish Sea: results from the first multi-centennial shell-based marine master chronology. Earth Planet Sci. Lett. 279 (3–4), 230–241.
Cook, G.T., Ascough, P.L., Bonsall, C., Hamilton, W.D., Russell, N., Sayle, K.L., Scott, E. M., Bownes, J.M., 2015. Best practice methodology for 14C calibration of marine and mixed terrestrial/marine samples. Quat. Geochronol. 27, 164–171.
Crothers, J.H., 1994. Student investigations on the populations structure of the common topshells, *Monodonta lineata*, on the Gore, Somerset. Field Stud. 8, 337–355.
Crothers, J.H., 2001. Common topshells: an introduction to the biology of Osilinus lineatus with notes on other species in the genus. Field Stud. 10, 115–160.
Crothers, J.H., 2003. Rocky shore snails as material for projects (with a key for their identification). Field Stud. 10, 601–634.
Díez-Urrutia, C., 2014. Distribución espacial de" Osilinus" spp.(Mollusca: Gasteropoda) en función de la amplitud de marea y el oleaje. Anales Universitarios de Etología 8, 7–14.
Domínguez-Villar, D., Fairchild, I.J., Baker, A., Wang, X., Edwards, R.L., Cheng, H., 2009. Oxygen isotope precipitation anomaly in the North Atlantic region during the 8.2 ka event. Geology 37, 1095–1098.
Donald, K.M., Preston, J., Williams, S.T., Reid, D.G., Winter, D., Alvarez, R., Buge, B., Hawkins, S.J., Templado, J., Spencer, H.G., 2012. Phylogenetic relationships elucidate colonization patterns in the intertidal grazers *Osilinus* philippi, 1847 and *Phorcus* risso, 1826 (Gastropoda: Trochidae) in the northeastern Atlantic Ocean and mediterranean sea. Mol. Phylogenet. Evol. 62 (1), 35–45.
England, J., Dyke, A.S., Coulthard, R.D., Mcneely, R., Aitken, A., 2013. The exaggerated radiocarbon age of deposit-feeding molluscs in calcareous environments. Boreas 42 (2), 362–373.
Fano, M.Á., 2019. The Mesolithic "Asturian" culture (North Iberia), one century on. Quat. Int. 515, 159–175.
Ferguson, J.E., Henderson, G.M., Fa, D.A., Finlayson, J.C., Charnley, N.R., 2011. Increased seasonality in the Western Mediterranean during the last glacial from limpet shell geochemistry. Earth Planet Sci. Lett. 308 (3–4), 325–333.
Fernandes, R., Dreves, A., 2017. Bivalves and radiocarbon. In: Allen, M.J. (Ed.), Molluscs in Archaeology: Methods, Approaches and Applications, pp. 365–381.
Fernandes, R., Bergemann, S., Hartz, S., Grootes, P.M., Nadeau, M.J., Melzner, F., Rakowski, A., Hüls, M., 2012. Mussels with meat: bivalve tissue-shell radiocarbon age differences and archaeological implications. Radiocarbon 54 (3–4), 953–965.
Fernandes, R., Millard, A.R., Brabec, M., Nadeau, M.J., Grootes, P., 2014. Food reconstruction using isotopic transferred signals (FRUITS): a Bayesian model for diet reconstruction. PloS One 9 (2), e87436.
Fernandes, R., Grootes, P., Nadeau, M.J., Nehlich, O., 2015. Quantitative diet reconstruction of a Neolithic population using a Bayesian mixing model (FRUITS): the case study of Ostorf (Germany). Am. J. Phys. Anthropol. 158 (2), 325–340.
Fernandes, R., Rinne, C., Nadeau, M.-J., Grootes, P., 2016. Towards the use of radiocarbon as a dietary proxy: establishing a first wide-ranging radiocarbon reservoir effects baseline for Germany. Environ. Archaeol. 21 (3), 285–294.
Fischer-Piette, E., 1941. Croissance, taille maxima et longevite possible de quelques animaux intercotidaux en fonction du milieu, vol. 21. Annales de l'Institut océanographique.
Fontanals-Coll, M., Subirà, M.E., Marín-Moratalla, N., Ruiz, J., Gibaja, J.F., 2014. From Sado Valley to Europe: Mesolithic dietary practices through different geographic distributions. J. Archaeol. Sci. 50, 539–550.
Forman, S.L., Polyak, L., 1997. Radiocarbon content of pre-bomb marine mollusks and variations in the 14C Reservoir age for coastal areas of the Barents and Kara Seas, Russia. Geophys. Res. Lett. 24 (8), 885–888.
García-Escárzaga, A., 2020. Paleoclima y aprovechamiento de recursos costeros durante el Mesolítico en la región cantábrica (N de Iberia). In: British Archaeological Reports Limited Internarcional Series, vol. 2976. BAR Publishing, Oxford.
García-Escárzaga, A., Gutiérrez-Zugasti, I., González-Morales, M.R., 2015. Análisis arqueomalacológico de la unidad estratigráfica 108 del conchero mesolítico de El Mazo (Llanes, Asturias): conclusiones socio-económicas y metodológicas. In: Gutiérrez Zugasti, I., Cuenca Solana, D., González-Morales, M.R. (Eds.), La Investigación Arqueomalacológica en la Península Ibérica: Nuevas Aportaciones. Nadir Ediciones, Santander, pp. 77–89.
García-Escárzaga, A., Gutiérrez-Zugasti, I., González-Morales, M.R., Cobo, A., 2017. Shells and Humans: Molluscs and Other Coastal Resources from the Earliest Human

Occupations at the Mesolithic Shell Midden of El Mazo (Asturias, Northern Spain) Papers from the Institute of Archaeology, vol. 27. Art. 3.
García-Escárzaga, A., Gutiérrez-Zugasti, I., Cobo, A., Cuenca-Solana, D., Martín-Chivelet, J., Roberts, P., González-Morales, M.R., 2019a. Stable oxygen isotope analysis of *Phorcus lineatus* (da Costa, 1778) as a proxy for foraging seasonality during the Mesolithic in northern Iberia. Archaeol. Anthropol. Sci. 11, 5631–5644.
García-Escárzaga, A., Gutiérrez-Zugasti, I., Schöne, B.R., Cobo, A., Martín-Chivelet, J., González-Morales, M.R., 2019b. Growth patterns of the topshell *Phorcus lineatus* (da Costa, 1778) in northern Iberia deduced from shell sclerochronology. Chem. Geol. 526, 49–61.
Guiry, E.J., Hillier, M., Richards, M.P., 2015. Mesolithic dietary heterogeneity on the European atlantic coastline: stable isotope insights into hunter-Gatherer diet and subsistence in the sado valley, Portugal. Curr. Anthropol. 56 (3), 460–470.
Gutiérrez Zugasti, I., González Morales, M.R., 2013. Intervención arqueológica en la cueva de El Mazo (Andrín, Llanes): campañas de 2009, 2010 y 2012, Excavaciones arqueológicas en Asturias 2007-2012. Gobierno del Principado de Asturias, Oviedo, pp. 159–167.
Gutiérrez Zugasti, I., Cuenca Solana, D., González Morales, M.R., García Escárzaga, A., Salazar Cañarte, S., Teira, L.C., Agudo Pérez, L., 2018b. Intervención Arqueológica en la cueva de El Mazo (Andrín, Llanes). Campañas de 2013, 2014, 2015 y 2016. In: Excavaciones arqueológicas en Asturias 2013-2016. Gobierno del Principado de Asturias, Oviedo, pp. 133–142.
Gutiérrez-Zugasti, I., Andersen, S.H., Araújo, A.C., Dupont, C., Milner, N., Monge-Soares, A.M., 2011. Shell midden research in Atlantic Europe: state of the art, research problems and perspectives for the future. Quat. Int. 239 (1–2), 70–85.
Gutiérrez-Zugasti, I., Cuenca-Solana, D., González-Morales, M.R., García-Moreno, A., Ortíz-Menéndez, J.E., Risseto, J., De Torres, T., 2013. Back to the Asturian: first result from the mesolithic shell midden site of el Mazo (Asturian, northern Spain). In: Daire, M.Y., Dupont, C., Baudry, A., Billard, C., Large, J.M., Lespez, L., Normand, E., Scarre, C. (Eds.), Ancient Maritime Communities and the Relationship between People and Environment along the European Atlantic Coasts. British Archaeological Reports Limited Internarcional Series 2570. Archaeopress, Oxford, pp. 483–490.
Gutiérrez-Zugasti, I., García-Escárzaga, A., Martín-Chivelet, J., González-Morales, M.R., 2015. Determination of sea surface temperatures using oxygen isotope ratios from *Phorcus lineatus* (Da Costa, 1778) in northern Spain: implications for paleoclimate and archaeological studies. Holocene 25 (1), 1002–1014.
Gutiérrez-Zugasti, I., Suárez-Revilla, R., Clarke, L.J., Schöne, B.R., Bailey, G.N., González-Morales, M.R., 2017. Shell oxygen isotope values and sclerochronology of the limpet *Patella vulgata* Linnaeus 1758 from northern Iberia: implications for the reconstruction of past seawater temperatures. Palaeogeogr. Palaeoclimatol. Palaeoecol. 475 (1), 162–175.
Gutiérrez-Zugasti, I., Rios-Garaizar, J., Marín-Arroyo, A.B., Rasines del Río, P., Maroto, J., Jones, J.R., Bailey, G.N., Richards, M.P., 2018a. A chrono-cultural reassessment of the levels VI–XIV from El Cuco rock-shelter: a new sequence for the Late Middle Paleolithic in the Cantabrian region (northern Iberia). Quat. Int. 474 (Part A), 44–55.
Hamilton, W.D., Krus, A.M., 2018. The myths and realities of Bayesian chronological modeling revealed. Am. Antiq. 83 (2), 187–203.
Hammer, S., Levin, I., 2017. Monthly Mean Atmospheric D14CO2 at Jungfraujoch and Schauinsland from 1986 to 2016, 10.11588/data/10100, heiDATA, vol. 2.
Hardy, K., Camara, A., Piqué, R., Dioh, E., Guèye, M., Diadhiou, H.D., Faye, M., Carré, M., 2016. Shellfishing and shell midden construction in the Saloum Delta, Senegal. J. Anthropol. Archaeol. 41, 19–32.
Hausmann, N., Meredith-Williams, M., Douka, K., Inglis, R.H., Bailey, G., 2019. Quantifying spatial variability in shell midden formation in the Farasan Islands, Saudi Arabia. PloS One 14 (1), e0217596.
Hawkins, S.J., Watson, D.C., Hill, A.S., Harding, S.P., Kyriakides, M.A., Hutchinson, S., Norton, T.A., 1989. A comparison of feeding mechanisms in microphagus, herbivorous, intertidal prosobranchs in relation to resources partitioning. J. Molluscan Stud. 55 (2), 151–165.
Heaton, T.J., Köhler, P., Butzin, M., Bard, E., Reimer, R.W., Austin, W.E.N., Bronk Ramsey, C., Grootes, P.M., Hughen, K.A., Kromer, B., Reimer, P.J., Adkins, J., Burke, A., Cook, M.S., Olsen, J., Skinner, L.C., 2020. Marine20—the marine radiocarbon age calibration curve (0–55,000 cal BP). Radiocarbon 62, 779–820.
Hoffman, J.S., Carlson, A.E., Winsor, K., Klinkhammer, G.P., LeGrande, A.N., Andrews, J. T., Strasser, J.C., 2012. Linking the 8.2 ka event and its freshwater forcing in the Labrador Sea. Geophys. Res. Lett. 39, L18703.
Keaveney, E.M., Reimer, P.J., 2012. Understanding the variability in freshwater radiocarbon reservoir offsets: a cautionary tale. J. Archaeol. Sci. 39 (5), 1306–1316.
Kendall, M.A., 1987. The Age and Size Structure of Some Northern Populations of the Trochid.
Lartaud, F., Emmanuel, L., de Rafelis, M., Pouvreau, S., Renard, M., 2010. Influence of food supply on the δ13C signature of mollusc shells: implications for palaeoenvironmental reconstitutions. Geo Mar. Lett. 30 (1), 23–34.
Lewis, C.F.M., Miller, A.A.L., Levac, E., Piper, D.J.W., Sonnichsen, G.V., 2012. Lake Agassiz outburst age and routing by Labrador Current and the 8.2 cal ka cold event. Quat. Int. 260, 83–97.
Little, C., Williams, G.A., Morritt, D., Perrins, J.M., Stirling, P., 1988. Foraging behaviour of *Patella vulgata* L. in an Irish sea-lough. J. Exp. Mar. Biol. Ecol. 120 (1), 1–21.
Lorrain, A., Paulet, Y.M., Chauvaud, L., Dunbar, R., Mucciarone, D., Fontugne, M., 2004. δ13C variation in scallop shells: increasing metabolic carbon contribution with body size? Geochem. Cosmochim. Acta 68 (17), 3509–3519.
Mangerud, J., Bondevik, S., Gulliksen, S., Hufthammer, A.K., Høisæter, T., 2006. Marine 14C reservoir ages for 19th century whales and molluscs from the North Atlantic. Quat. Sci. Rev. 25 (23–24), 3228–3245.
Mannino, M., Thomas, K., Leng, M., Piperno, M., Tusa, S., Tagliacozzo, A., 2007. Marine resources in the Mesolithic and Neolithic at the Grotta dell'Uzzo (Sicily): evidence from isotope analyses of marine shells. Archaeometry 49 (1), 117–133.
Mary, Y., Eynaud, F., Colin, C., Rossignol, L., Brocheray, S., Mojtahid, M., Garcia, J., Peral, M., Howa, H., Zaragosi, S., Cremer, M., 2017. Changes in Holocene meridional circulation and poleward Atlantic flow: the Bay of Biscay as a nodal point. Clim. Past 13, 201–216.
McConnaughey, T.A., Gillikin, D.P., 2008. Carbon isotopes in mollusk shell carbonates. Geo Mar. Lett. 28, 287–299.
Milano, S., Schöne, B.R., Gutiérrez-Zugasti, I., 2020. Oxygen and carbon stable isotopes of Mytilus galloprovincialis Lamarck, 1819 shells as environmental and provenance proxies. Holocene 30, 65–76.
Milner, N., Craig, O.E., Bailey, G.N., 2007. Shell Middens in Atlantic Europe. Oxbow Books Ltd, Oxford.
Moreno, A., López-Merino, L., Leira, M., Marco-Barba, J., González-Sampériz, P., Valero-Garcés, B.L., López-Sáez, J.A., Santos, L., Mata, P., Ito, E., 2011. Revealing the last 13,500 years of environmental history from the multiproxy record of a mountain lake (Lago Enol, northern Iberian Peninsula). J. Paleolimnol. 46, 327–349.
Nuñez de la Fuente, S., 2018. Dinámicas socio-ecológicas, resilencia y vulnerabilidad en un paisaje atlántico montañoso: la región cantábrica durante el Holoceno. Universidad de Cantabria, Santander (Unpublish PhD dissertation).
Ortlieb, L., Vargas, G., Saliège, J.-F., 2011. Marine radiocarbon reservoir effect along the northern Chile–southern Peru coast (14–24 S) throughout the Holocene. Quat. Res. 75 (1), 91–103.
Perona, J., Canals, À., Cardellach, E., 2018. Zn-Pb mineralization associated with salt diapirs in the Basque-Cantabrian basin, northern Spain: geology, geochemistry, and Genetic model. Econ. Geol. 113, 1133–1159.
Poppe, G.T., Goto, Y., 1991. Polyplacophora, Caudofoveata, Solenogastra, Gastropoda). In: European Seashells, vol. I. Verlag Christa Hemmen, Germany.
Reimer, P.J., Austin, W.E.N., Bard, E., Bayliss, A., Blackwell, P.G., Bronk Ramsey, C., Butzin, M., Cheng, H., Edwards, R.L., Friedrich, M., Grootes, P.M., Guilderson, T.P., Hajdas, I., Heaton, T.J., Hogg, A.G., Hughen, K.A., Kromer, B., Manning, S.W., Muscheler, R., Palmer, J.G., Pearson, C., van der Plicht, J., Reimer, R.W., Richards, D.A., Scott, E.M., Southon, J.R., Turney, C.S.M., Wacker, L., Adolphi, F., Büntgen, U., Capano, M., Fahrni, S.M., Fogtmann-Schulz, A., Friedrich, R., Köhler, P., Kudsk, S., Miyake, F., Olsen, J., Reinig, F., Sakamoto, M., Sookdeo, A., Talamo, S., 2020. The IntCal20 northern hemisphere radiocarbon age calibration curve (0–55 cal kBP). Radiocarbon 62, 725–757.
Risebrobakken, B., Jansen, E., Andersson, C., Mjelde, E., Hevrøy, K., 2003. A high-resolution study of Holocene paleoclimatic and paleoceanographic changes in the Nordic Seas. Paleoceanography 18.
Rohling, E.J., Pälike, H., 2005. Centennial-scale climate cooling with a sudden cold event around 8,200 years ago. Nature 434, 975.
Romanek, C.S., Grossman, E.L., Morse, J.W., 1992. Carbon isotopic fractionation in synthetic aragonite and calcite: effects of temperature and precipitation rate. Geochem. Cosmochim. Acta 56, 419–430.
Rossi, C., Bajo, P., Lozano, R.P., Hellstrom, J., 2018. Younger Dryas to Early Holocene paleoclimate in Cantabria (N Spain): Constraints from speleothem Mg, annual fluorescence banding and stable isotope records. Quat. Sci. Rev. 192, 71–85.
Rossi, C., Bajo, P., Lozano, R.P., Hellstrom, J., 2018. Younger Dryas to Early Holocene paleoclimate in Cantabria (N Spain): Constraints from speleothem Mg, annual fluorescence banding and stable isotope records. Quat. Sci. Rev. 192, 71–85.
Russell, N., Cook, G.T., Ascough, P., Barrett, J.H., Dugmore, A., 2011. Species specific marine radiocarbon reservoir effect: a comparison of ΔR values between Patella vulgata (limpet) shell carbonate and Gadus morhua (Atlantic cod) bone collagen. J. Archaeol. Sci. 38 (5), 1008–1015.
Schulting, R.J., Richards, M.P., 2001. Dating women and becoming farmers: new palaeodietary and AMS dating evidence from the Breton mesolithic Cemeteries of Téviec and hoëdic. J. Anthropol. Archaeol. 20 (3), 314–344.
Scott, E.M., Cook, G.T., Naysmith, P., 2007. Error and uncertainty in radiocarbon measurements. Radiocarbon 49 (2), 427–440.
Smith, A.C., Wynn, P.M., Barker, P.A., Leng, M.J., Noble, S.R., Tych, W., 2016. North Atlantic forcing of moisture delivery to Europe throughout the Holocene. Sci. Rep. 6, 24745.
Soares, A.M.M., Dias, J.M.A., 2006. Coastal upwelling and radiocarbon—Evidence for temporal fluctuations in ocean reservoir effect off Portugal during the holocene. Radiocarbon 48, 45–60.
Soares, A.M.M., Gutiérrez-Zugasti, I., González-Morales, M., Martins, J.M.M., Cuenca-Solana, D., Bailey, G.N., 2016. Marine radiocarbon reservoir effect in late pleistocene and early Holocene coastal waters off northern Iberia. Radiocarbon 58 (4), 869–883.
Solomon, C.T., Weber, P.K., Joseph J Cech, J., Ingram, B.L., Conrad, M.E., Machavaram, M.V., Pogodina, A.R., Franklin, R.L., 2006. Experimental determination of the sources of otolith carbon and associated isotopic fractionation. Can. J. Fish. Aquat. Sci. 63, 79–89.
Sousa, R., Delgado, J., González, J.A., Freitas, M., Henriques, P., Ray, S., 2018. Marine snails of the genus Phorcus: biology and ecology of sentinel species for human impacts on the rocky shores. In: Ray, S. (Ed.), Biological Resources of Water. IntechOpen, Croatia, pp. 141–167.
Stuiver, M., Braziunas, T.F., 1993. Modeling atmospheric 14C influences and 14C ages of marine samples to 10,000 BC. Radiocarbon 35 (1), 137–189.
Stuiver, M., Polach, H.A., 1977. Discussion reporting of 14C data. Radiocarbon 19 (3), 355–363.
Stuiver, M., Pearson, G.W., Braziunas, T., 1986. Radiocarbon age calibration of marine samples back to 9000 cal yr BP. Radiocarbon 28 (2B), 980–1021.

Teller, J.T., Leverington, D.W., Mann, J.D., 2002. Freshwater outbursts to the oceans from glacial Lake Agassiz and their role in climate change during the last deglaciation. Quat. Sci. Rev. 21, 879–887.
Thomas, E.R., Wolff, E.W., Mulvaney, R., Steffensen, J.P., Johnsen, S.J., Arrowsmith, C., White, J.W.C., Vaughn, B., Popp, T., 2007. The 8.2ka event from Greenland ice cores. Quat. Sci. Rev. 26, 70–81.
Ward, G.K., Wilson, S.R., 1978. Procedures for comparing and combining radiocarbon age determinations: a critique. Archaeometry 20 (1), 19–31.
Weninger, B., Edinborough, K., Bradtmöller, M., Collard, M., Crombé, P., Danzeglocke, U., Holst, D., Jöris, O., Niekus, M., Shennan, S., 2009. A radiocarbon database for the mesolithic and early neolithic in northwest Europe, chronology and evolution within the mesolithic of north-west Europe. In: Crombé, P.Van, Strydonck, M., Sergant, J., Boudin, M., Bats, M. (Eds.), Chronology and Evolution within the Mesolithic of North-West Europe. Scholars Publishing, Cambridge, pp. 143–176.
Yoneda, M., Tanaka, A., Shibata, Y., Morita, M., Uzawa, K., Hirota, M., Uchida, M., 2002. Radiocarbon marine reservoir effect in human remains from the kitakogane site, hokkaido, Japan. J. Archaeol. Sci. 29, 529–536.
Zilhão, J., Angelucci, D.E., Badal-García, E., d'Errico, F., Daniel, F., Dayet, L., Douka, K., Higham, T.F.G., Martínez-Sánchez, M.J., Montes-Bernárdez, R., Murcia-Mascarós, S., Pérez-Sirvent, C., Roldán-García, C., Vanhaeren, M., Villaverde, V., Wood, R., Zapata, J., 2010. Symbolic use of marine shells and mineral pigments by Iberian Neandertals. Proc. Natl. Acad. Sci. Unit. States Am. 107, 1023–1028.